THE JOURNAL OF BIOLOGICAL CHEMISTRY
Vol. 259, no. 1, Issue of January 10, pp. 255-264, 1984
Printed in U.S.A.

Kinetic Properties and Sites of Autophosphorylation of the Partially Purified Insulin Receptor from Hepatoma Cells*

(Received for publication, June 20, 1983)

Morris F. White, Hans-Ulrich Haring‡, Masato Kasuga§, and C. Ronald Kahn¶

From the Research Division, Joslin Diabetes Center, and the Department of Medicine, Brigham and Women's Hospital and Harvard Medical School, Boston, Massachusetts 02215

Autophosphorylation of the insulin receptor was studied using a glycoprotein fraction solubilized and purified partially from the rat hepatoma cell line, Fao. Incubation of this receptor preparation with [γ-^{32}P] ATP, Mn^{2+}, and insulin yielded a single insulin-stimulated phosphoprotein of M_r = 95,000 which corresponds to the β-subunit of the insulin receptor. At 22 °C, incorporation of ^{32}P was half-maximal at 30 s and about 90% complete after 2 min. At steady state, about 200 pmol of ^{32}P were incorporated per mg of protein; this value corresponded to about 2 molecules of phosphate per insulin binding site estimated from Scatchard plots. Insulin increased the V_{max} for autophosphorylation of the insulin receptor kinase nearly 20-fold with no effect on the K_m for ATP. Mn^{2+} stimulated autophosphorylation by decreasing the K_m of the kinase for ATP, whereas Mg^{2+} had no effect. Dilution of the insulin receptor over a 10-fold concentration range did not decrease the rate of autophosphorylation suggesting that it may occur by an intramolecular mechanism. When the phosphorylated β-subunit of the insulin receptor was digested with trypsin, at least 5 phosphopeptides could be separated by high performance liquid chromatography on a μBondapak C_{18} reverse-phase column. Insulin stimulated the phosphorylation of all sites. These phosphate acceptor sites varied in their rate and degree of phosphorylation. Phosphopeptides pp4 and pp5 were phosphorylated very rapidly and reached steady state within 20 s, whereas phosphorylation of pp1 and pp2 required several minutes to reach steady state.

We have shown that insulin stimulates phosphorylation of the M_r = 95,000 (β) subunit of the insulin receptor in intact cells (1, 2, 4)[1] and several cell-free systems (4-8).[1] In the intact cell, insulin increases the amount of phosphoserine, phosphothreonine, and phosphotyrosine in the receptor (1, 2). After solubilization and purification, insulin stimulates phosphorylation of tyrosine residues in both the receptor (5-7) and other proteins (8). Similar findings have been made in other laboratories using different systems (9-16). The insulin-stimulated protein kinase co-purifies with the insulin receptor during immunopurification with anti-insulin receptor antibodies (7, 13) and affinity chromatography on insulin-Sepharose (7). Furthermore, the insulin receptor can be labeled using ATP affinity reagents (14-16). Together, these findings suggest that the insulin receptor is a tyrosine-specific protein kinase.

Tyrosine phosphorylation may be involved in the regulation of cellular growth and metabolism. In addition to the insulin receptor, the receptors for epidermal growth factor (17-21) and platelet-derived growth factor (22-24) appear to be hormone-sensitive tyrosine kinases. Cellular transformation induced by infection with the Rous sarcoma virus also seems to be mediated through the tyrosine kinase activity of its gene product, pp60$^{v\text{-}src}$ (25). The physiologic role of autophosphorylation at tyrosine residues is unknown, although it may regulate the catalytic activity of tyrosine kinases (26) as has been suggested for some serine and threonine kinases (27).

In this report, we characterize the autophosphorylation reaction of the insulin receptor partially purified from the hepatoma cell Fao. We find that the reaction is under dual regulation. Insulin stimulates autophosphorylation by increasing the V_{max}, whereas Mn^{2+} activates this reaction by decreasing the K_m for ATP. Autophosphorylation of the insulin receptor kinase appears to occur at several distinct sites *in vitro* as determined by the separation of tryptic phosphopeptides using reverse-phase HPLC.[2] These sites show different time courses suggesting that autophosphorylation of one site may stimulate the autophosphorylation of other sites. Autophosphorylation of the β-subunit of the insulin receptor at tyrosine residues may be the first molecular event to signal intracellularly the binding of insulin on the external surface of the plasma membrane.

EXPERIMENTAL PROCEDURES AND RESULTS[3]

The Time Course of Insulin Receptor Autophosphorylation—An autoradiogram showing the time course of *in vitro* auto-

* This work has been supported in part by Grant AM31036 from the Institute of Health and Human Development, National Institutes of Health, United States Public Health Service. The costs of publication of this article were defrayed in part by the payment of page charges. This article must therefore be hereby marked "*advertisement*" in accordance with 18 U.S.C. Section 1734 solely to indicate this fact.

‡ Present address, Institut fur Diabetesforschung, Platz 1, 8 Munchen 40, Federal Republic of Germany.

§ Present address, The Third Department of Internal Medicine, Faculty of Medicine, University of Tokyo, 7-3-1 Hongo, Bunkyo-ku, Tokyo, Japan.

¶ To whom reprint requests should be addressed.

[1] H.-U. Haring, M. Kasuga, M. F. White, M. Crettaz, and C. R. Kahn, submitted to *Biochemistry*.

[2] The abbreviations used are: HPLC, high performance liquid chromatography; DTT, dithiothreitol; Hepes, 4-(2-hydroxyethyl)-1-piperazineethanesulfonic acid; SDS, sodium dodecyl sulfate; PAGE, polyacrylamide gel electrophoresis; pp60$^{v\text{-}src}$, gene product of the Rous sarcoma virus; PMSF, phenylmethylsulfonyl fluoride.

[3] Portions of this paper (including "Experimental Procedures," part of "Results," and Figs. 1-3, 8, and 9) are presented in miniprint at the end of this paper. Miniprint is easily read with the aid of a standard magnifying glass. Full size photocopies are available from the Journal of Biological Chemistry, 9650 Rockville Pike, Bethesda, MD 20814. Request Document No. 83M-1731, cite the authors, and include a check or money order for $5.20 per set of photocopies. Full size photocopies are also included in the microfilm edition of the Journal that is available from Waverly Press.

phosphorylation of the β-subunit of the insulin receptor-kinase is shown in Fig. 4. In the absence of insulin, autophosphorylation occurred slowly. Insulin (100 nM) stimulated the incorporation of ^{32}P from [γ-^{32}P]ATP into the β-subunit of the receptor. Within 30 s, autophosphorylation of the insulin-stimulated receptor reached 50% of maximum and a steady state value was reached after about 10 min (Fig. 5*A*). Maximal phosphorylation varied between preparations of receptor; in the experiments reported here, about 200 pmol of ^{32}P were incorporated per mg of protein. This steady state level of autophosphorylation corresponds to about 2 molecules of ^{32}P incorporated per insulin binding site estimated from a Scatchard plot (Fig. 1).

Fig. 5, *B–H* shows the HPLC phosphopeptide maps corresponding to the time course of autophosphorylation of the β-subunit shown in Fig. 5*A*. The phosphopeptides have been numbered consecutively with the omission of pp3 which was not resolved in this experiment due to the collection of eluant in 1-min fractions (see below). Phosphorylation of each site did not occur with an identical time course (Fig. 5, *B–H* and Fig. 6). Only tryptic peptides pp4 and pp5 were detected after 5 s of incubation with [γ-^{32}P]ATP and reached apparent steady state levels after only 20 s (Fig. 6). These rapid sites of autophosphorylation contrasted with the slower sites (pp1 and pp2) that were detectable only after longer incubation intervals and reached steady state in 5–10 min (Fig. 6). The phosphorylation of pp2 appeared to lag slightly, whereas pp1 lagged markedly relative to the phosphorylation of pp4 and pp5. Although the occurrence of multiple phosphopeptides could be due to incomplete digestion of the β-subunit by trypsin, our kinetic results are consistent with the notion that the phosphopeptides resolved by HPLC are unique sites of autophosphorylation. Additional phosphopeptides eluted after 40 min appeared to be phosphorylated relatively slowly (Fig. 5, *F–H*).

The Effect of Receptor Concentration on Autophosphorylation of the β-Subunit—When concentrations of all other components in the reaction mixture were unchanged, autophosphorylation of the insulin receptor was proportional to the amount of protein used in the assay (Fig. 7, *left*). The slope of the line has a value of 95 pmol of ^{32}P per mg of protein per min which agrees with the value shown in Fig. 5*A* at the corresponding time interval. These results suggest that nonspecific hydrolysis of ATP which could interfere with the kinetic studies did not occur to a significant extent with increasing protein concentrations because ATPase activity should cause a nonlinear relation between protein concentration and autophosphorylation. These results also suggest that the decreasing ratio of protein to Triton X-100 does not affect autophosphorylation. Furthermore, when the protein concentration was constant at 40 μg/μl and the Triton X-100 concentration was varied between of 0.02% and 0.1%, the rate of autophosphorylation measured during a 30-s time interval was not affected (data not shown).

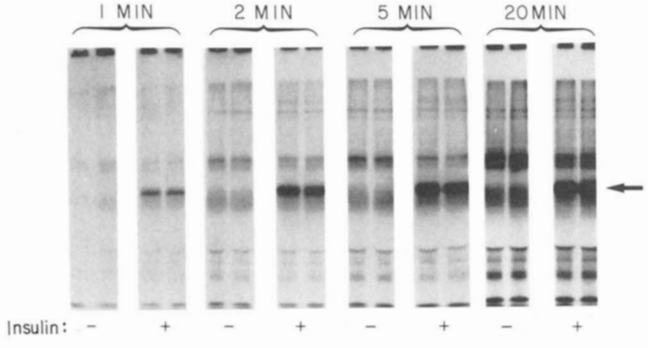

FIG. 4. **A time course of insulin receptor autophosphorylation.** Duplicate portions of wheat germ agglutinin-purified insulin receptor (3.4 μg) were incubated for 1 h in the presence (+) or absence (−) of 100 nM insulin. Then, 50 μM [γ-^{32}P]ATP was added for the indicated time intervals. The reactions were terminated by heating with DTT-containing Laemmli sample buffer for 2 min. The proteins were separated by SDS-PAGE. The *arrow* indicates the expected migration of the β-subunit.

Autophosphorylation of the β-subunit of the insulin receptor could occur by an intramolecular reaction in which the catalytic domain and the phosphorylation sites are located on the same molecular aggregate or by an intermolecular reaction in which the catalytic domains and phosphorylation sites reside on separate receptor molecules. The velocity of phosphorylation by the former mechanism should be independent of the concentration of the receptor, whereas the concentration of receptor should affect the rate of phosphorylation which occurs by an intermolecular reaction (37, 38). When the amount of lectin-purified protein added to the reaction mixture was maintained at a constant level, but its concentration was decreased by increasing the volume of the phosphorylation reaction mixture, no significant effect on the approximate initial rate of autophosphorylation measured during a 1-min interval was observed (Fig. 7, *right*). Therefore, autophosphorylation of the insulin receptor may occur by an intramolecular reaction, a result which suggests that only receptors occupied with insulin will undergo stimualted autophosphorylation.

The Effect of the ATP Concentration on the Sites of Autophosphorylation of the Insulin Receptor—The velocity curves of insulin-stimulated autophosphorylation were sigmoidal with respect to the ATP concentration (Fig. 8). Mn^{2+}, within the concentration interval of 0–5 mM, was an essential activator of autophosphorylation, whereas higher concentrations of Mn^{2+} were inhibitory (Fig. 9). These results are consistent with the complex kinetic behavior reported for metal-activated enzymes (42–44) or may arise from a regulatory phenomenon involving activation of the receptor by autophosphorylation. However, this kinetic analysis should be viewed cautiously because autophosphorylation of the insulin receptor occurs at multiple sites with distinct time courses and apparently by an intramolecular reaction.

HPLC tryptic peptide maps of the phosphorylated β-subunit obtained at various ATP concentrations after the incubation with 100 nM insulin are shown in Fig. 10, *top*. Phosphorylation of pp2 through pp5 was detected in this experiment, whereas the 1-min interval was not long enough to observe pp1. The improved resolution was due presumably to the collection of fractions during 24-s time intervals (compare with Fig. 5, *B–H*). In some experiments, pp2 was separated into 2 peaks (2*a* and 2*b*), but for the present study, these peaks were analyzed together. Plotting the total radioactivity associated with each peptide fragment against the ATP concentration yielded kinetic curves describing the phosphorylation of pp2, pp3, pp4, and pp5 (Fig. 10, *middle*). Like the phosphorylation of the entire receptor, sigmoidal curves were obtained for pp2, pp3, and pp4. However, the curve for pp5 was hyperbolic. Although the phosphorylation of pp4 and pp5 has probably reached steady state during the 1-min reaction (Fig. 6), the different shape of the curves for pp4 and pp5 supports our conclusion that these phosphopeptides represent distinct phosphorylation sites on the β-subunit. As emphasized by the relative curves in Fig. 10, *bottom*, the phosphorylation of pp5 precedes the phosphorylation of the other peptides. These results, in addition to the time courses shown before (Fig. 6), suggest that autophosphorylation of pp5 may facilitate subsequent phosphorylation of the receptor at the

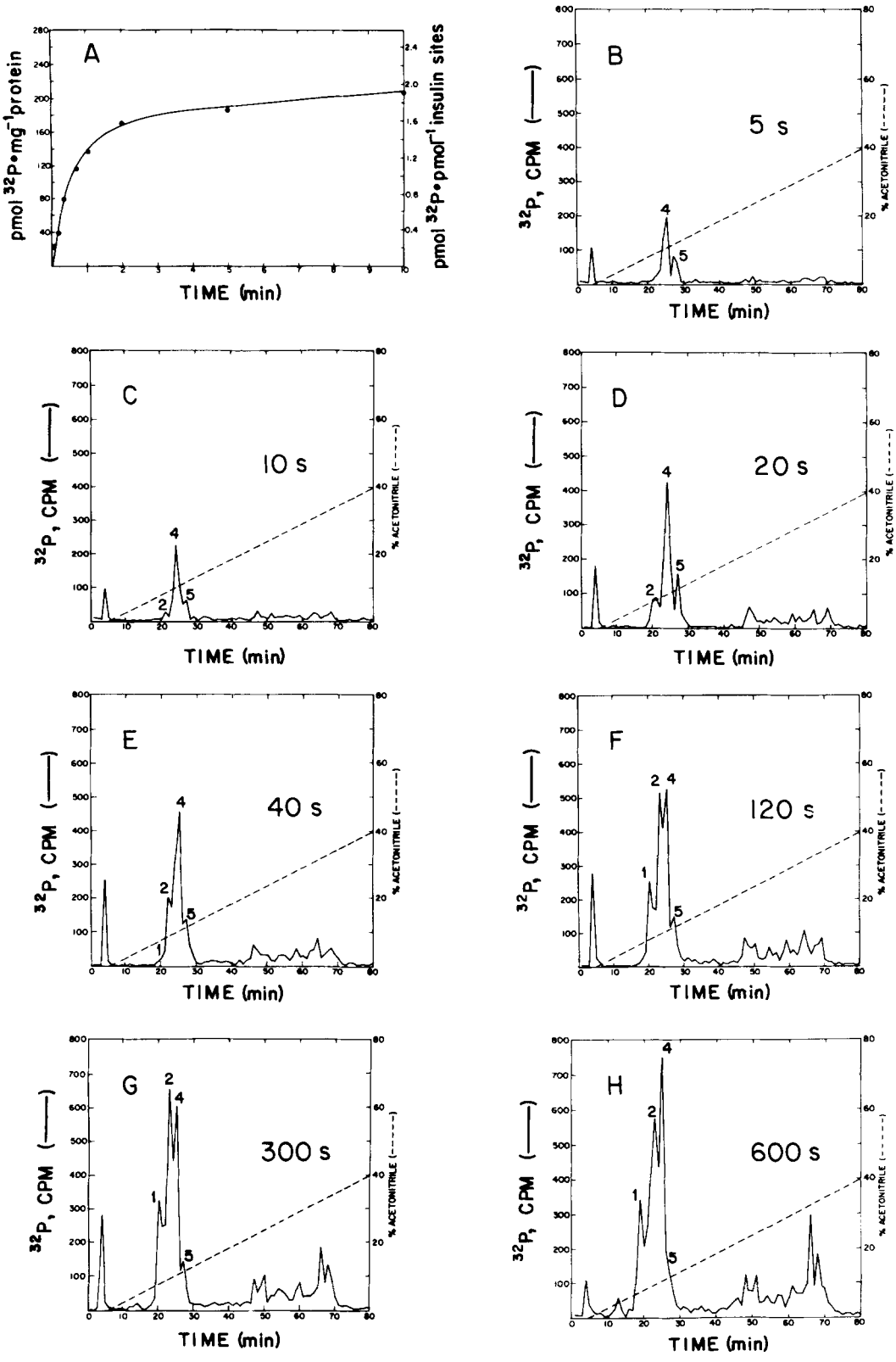

FIG. 5. **A time course of insulin-stimulated autophosphorylation of the β-subunit and reverse-phase HPLC separation of the corresponding phosphopeptides obtained by trypsin digestion.** The insulin receptor (4 μg) was incubated in a 50-μl reaction mixture containing 100 nM insulin and 10 mM Mn^{2+} for 1 h and then 50 μM [γ-^{32}P]ATP was added for the indicated time intervals. The β-subunit, located by autoradiography, was excised from the gel and the radioactivity in the gel fragment was determined by scintillation counting. The gel fragments obtained at each time interval of incubation (*B*, 5 s; *C*, 10 s; *D*, 20 s; *E*, 40 s; *F*, 120 s; *G*, 300 s; *H*, 600 s) were digested with trypsin for 24 h and the eluted phosphopeptides were separated by HPLC. Fractions (1 ml) were collected at 1-min intervals and the chromatogram obtained by measuring the radioactivity is represented by the *solid lines* (——). pp3 was not resolved between pp2 and pp4 owing to the collection of fractions during 1-min time intervals. The linear gradient of acetonitrile is indicated by the *dashed line* (- - -).

other sites and possibly other substrates (26).

The Effect of Insulin Concentration on the Phosphorylation of the Insulin Receptor—Insulin stimulated autophosphorylation of the β-subunit about 20-fold; half-maximal stimulation occurred at about 5 nM insulin with a slight inhibition detected above 100 nM (Fig. 11, *top*). Analysis of a series of sigmoidal velocity curves obtained at various insulin concentrations suggests that insulin stimulated autophosphorylation by increasing the V_{max} of the reaction with no effect on the K_m for ATP (Table I).

After a 1-min incubation with 50 μM [γ-^{32}]ATP, insulin stimulated the incorporation of ^{32}P into pp2–pp5 of the insulin receptor (Fig. 11, *middle*). A dose response curve for each phosphopeptide measured between 1 and 1000 nM insulin is shown in Fig. 11, *bottom*. Summation of the radioactivity associated with each peak yielded the following order of stimulation relative to the values at 1 nM and 100 nM insulin: pp2 (9.1-fold) > pp4 (7.7-fold) > pp3 (6.7-fold) > pp5 (4.4-fold). Phosphorylation of pp1 was too slow to detect after a

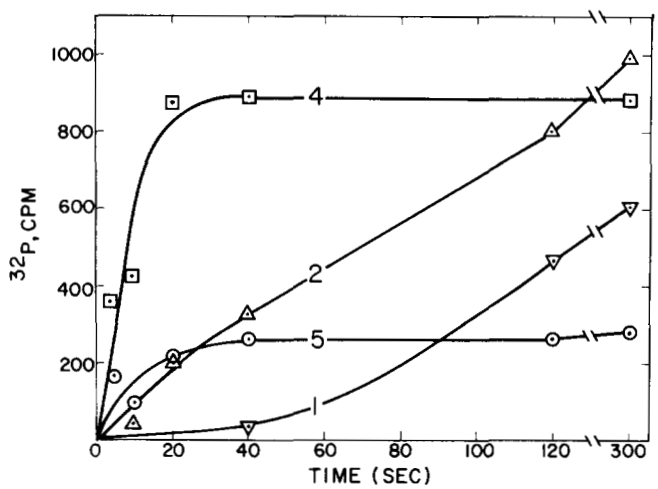

FIG. 6. **A time course of autophosphorylation of several tryptic phosphopeptides obtained from the β-subunit of the insulin receptor.** The phosphopeptides, pp1 (▽), pp2 (△), pp4 (□), and pp5 (○) identified in Fig. 5 were quantitated by determining the approximate radioactivity associated with each peak. Where baseline resolution was not complete, the radioactivity was divided equally between each peak.

TABLE I

The effect of insulin on the observed kinetic parameters for insulin receptor autophosphorylation

Insulin receptor (3.6 μg) was incubated with the indicated concentrations of insulin for 1 h at room temperature in the standard reaction mixture containing 3.5 mM Mn^{2+}. Autophosphorylation was initiated by adding [γ-^{32}P]ATP at the following concentrations: 2.5, 5.0, 10.0, 20.0, 40.0, 60.0, and 200 μM. After a 1-min incubation, the reaction was stopped, the proteins were separated by SDS-PAGE, and the β-subunit was localized by autoradiography. The gel fragments corresponding to these regions were excised and the radioactivity was determined by scintillation counting. The kinetic parameters ± S.E. were determined by fitting the data to Equation 2.

[Insulin]	K_m (±S.E.) (ATP)	V_{max} (±S.E.)
nM	*μM*	*pmol/mg protein/min*
0.1	46 ± 4	13 ± 1
1.0	53 ± 4	25 ± 2
10.0	51 ± 5	70 ± 9
100.0	58 ± 8	203 ± 33

TABLE II

The effect of ATP on the observed kinetic parameters for Mn^{2+} stimulation of receptor autophosphorylation

See the legend to Fig. 12 for experimental details. The kinetic parameters ± S.E. were determined by fitting the data to Equation 2.

[ATP]	K_m (±S.E.) (Mn^{2+})	V_{max} (±S.E.)
μM	*mM*	*pmol/mg protein/min*
5	1.6 ± 0.2	11 ± 1
10	2.7 ± 0.8	32 ± 6
25	3.6 ± 0.5	106 ± 10
75	2.5 ± 1.0	202 ± 60
100	0.48 ± 0.09	158 ± 10
150	0.37 ± 0.12	164 ± 16
200	0.12 ± 0.06	149 ± 11

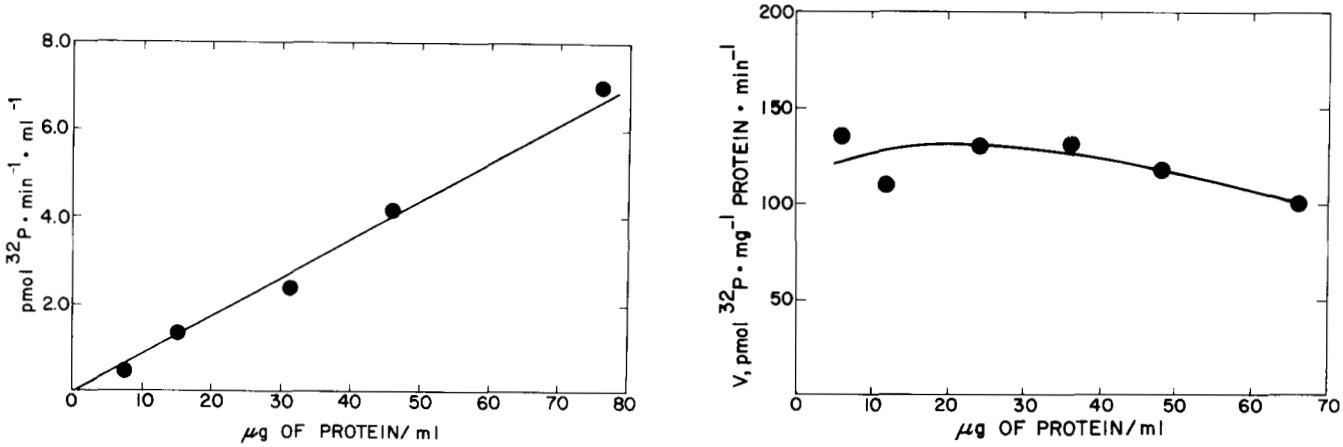

FIG. 7. **The effect of protein concentration on the rate of autophosphorylation of the β-subunit.** *Left*, the amount of protein added to a constant volume of phosphorylation reaction mixture (50 μl) containing 100 nM insulin and 5 mM Mn^{2+} was varied between 0.35 and 3.5 μg and incubated for 1 h. The ^{32}P incorporated into the β-subunit after a 1-min incubation following the addition of 50 μM [γ-^{32}P]ATP is shown. *Right*, fixed amount of insulin receptor (3.6 μg) was incubated for 1 h with 100 nM insulin and 5 mM Mn^{2+} in an increasing reaction volume so that the protein concentration decreased from 66 μg/ml to 6.6 μg/ml. [γ-^{32}P]ATP was added to a final concentration of 500 μM for 1 min. Each reaction mixture was stopped by heating to 100 °C for 3 min and concentrated by lyophilization. The residue was dissolved in Laemmli sample buffer and the proteins were separated by SDS-PAGE. The β-subunit was identified by autoradiography and the radioactivity was determined by scintillation counting.

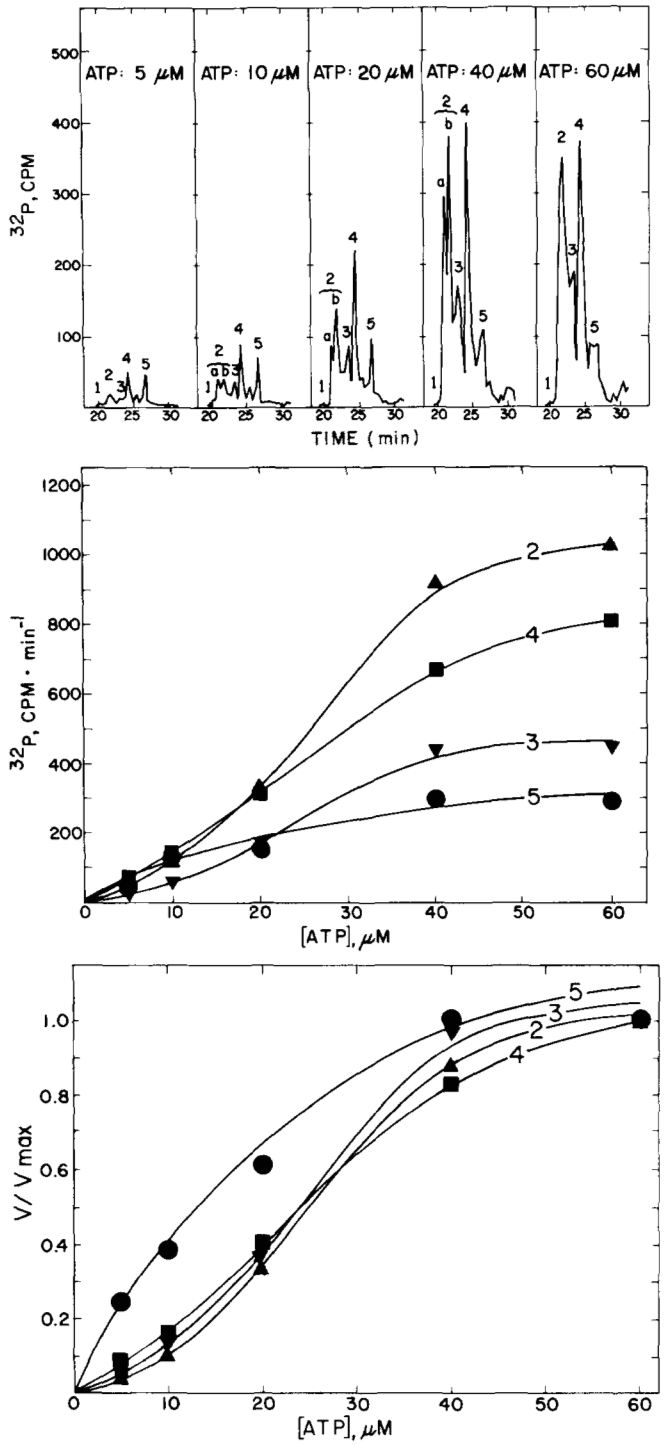

FIG. 10. **The effect of ATP concentration on the HPLC tryptic peptide maps.** Solubilized insulin receptor (4 μg) was incubated with 100 nM insulin and 5.0 mM Mn^{2+} for 1 h followed by the addition of [γ-^{32}P]ATP at the concentrations of ATP indicated on the figure. After 1 min, the reaction was terminated by heating to 100 °C for 2 min and the proteins were separated by SDS-PAGE. The phosphorylated β-subunit of the insulin receptor was identified by autoradiography. The gel fragments containing the β-subunit were incubated with trypsin for 24 h. *Top*, the phosphopeptides obtained at each ATP concentration were separated by HPLC and the relevant regions of the chromatograms are shown. The acetonitrile gradient used was 0% (5 min) and 0%–70% (75 min). *Middle*, the radioactivity associated with pp2 (▲), pp3 (▼), pp4 (■), and pp5 (●) was determined and plotted against the ATP concentration. *Bottom*, a replot was constructed to show the relative ^{32}P incorporation into peptides pp2–pp5 normalized to the maximum phosphorylation obtained for each peptide at 60 μM ATP.

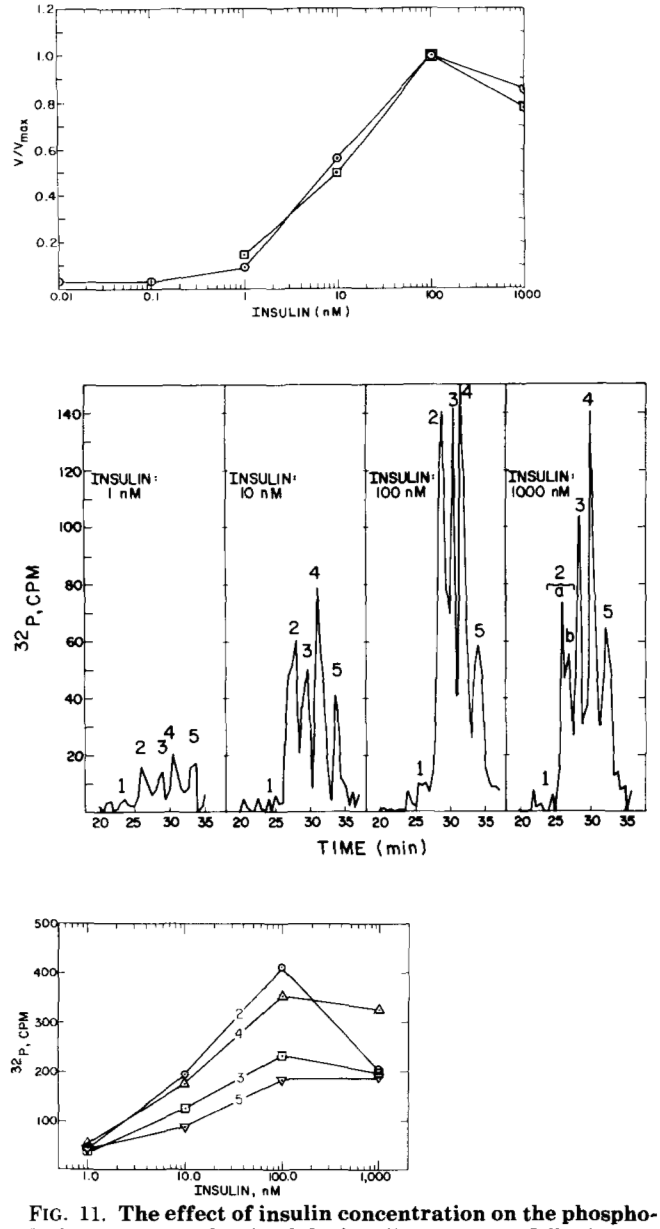

FIG. 11. **The effect of insulin concentration on the phosphorylation of the β-subunit of the insulin receptor.** Following a 1-h incubation with 5 mM Mn^{2+} and the indicated concentrations of insulin, the solubilized insulin receptor (3.6 μg) was incubated during a 1-min time interval with 50 μM [γ-^{32}P]ATP. The β-subunit was separated by PAGE and its position was identified by autoradiography. The associated radioactivity was quantitated by scintillation counting. *Top*, ⊙, the insulin dose response curve is plotted relative to the maximum velocity of phosphorylation which occurred at 100 nM insulin (82 pmol of ^{32}P/mg of protein/min). *Middle*, the gel fragments obtained from the experiments with 1 nM, 10 nM, 100 nM, and 1000 nM insulin were digested with trypsin for 24 h. The phosphopeptides, pp2–pp5, were separated by HPLC and the corresponding chromatograms of the relevant regions are shown. The acetonitrile gradient used was 0% (5 min) and 0%–70% (75 min). *Bottom*, the radioactivity associated with pp2 (⊙), pp3 (⊡), pp4 (△), and pp5 (▽) are plotted as a function of the insulin concentration. For comparison, the insulin dose response curve obtained by adding the radioactivity associated with each peak is compared to the curve obtained from the original gel fragments (*far left*, ⊡).

1-min incubation (Fig. 6). When the insulin concentration was raised to 1000 nM, the phosphorylation of pp2 was inhibited by approximately 50%. Reconstruction of the relative dose response curve from the individual peptides suggests that the decreased incorporation of ^{32}P into the intact β-subunit obtained at 1000 nM insulin was due entirely to the inhibition

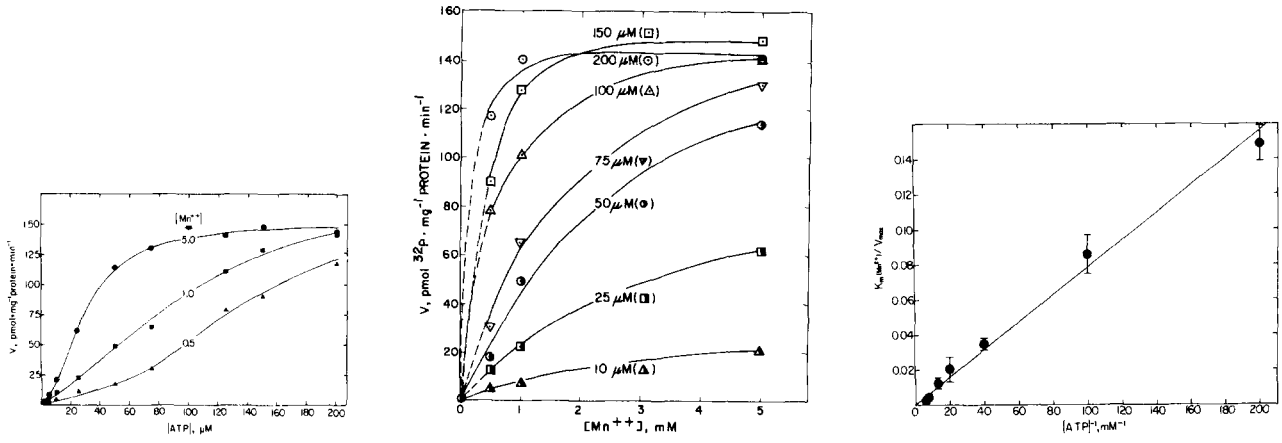

FIG. 12. **Kinetic curves of insulin-stimulated receptor autophosphorylation at various concentrations of Mn^{2+}.** *Solubilized insulin receptor* (3.4 μg) was incubated with 100 nM insulin and 0.5, 1.0, or 5.0 mM Mn^{2+} for 1 h followed by the addition of [γ-^{32}P]ATP for 30 s at the indicated concentrations. The reaction was terminated by heating to 100 °C for 2 min and the proteins were separated by SDS-PAGE. The phosphorylated β-subunit of the insulin receptor was identified by autoradiography and the radioactivity in the corresponding gel fragment was quantitated by scintillation counting. *Left,* kinetic curves of Mn^{2+}-stimulated insulin receptor autophosphorylation as a function of the [ATP]. *Center,* these reaction velocities are replotted as a function of the total [Mn^{2+}] used in the assay. The [ATP] (μM) is shown on the figure and a statistical analysis of these data is provided in Table II. *Right,* K_m (Mn^{2+})/V_{max}, calculated from the values of the kinetic parameters in Table II, is plotted against the corresponding reciprocal of the ATP concentration.

of phosphorylation of pp2 (Fig. 11, *top*).

The Relation between ATP and Mn^{2+} for Autophosphorylation—In contrast to the effect of insulin on autophosphorylation which occurs by increasing the V_{max} (Table I), the sigmoidal velocity curves shown in Fig. 12 (*left*) indicate that Mn^{2+} stimulated the *in vitro* autophosphorylation reaction by decreasing the concentration of ATP necessary to obtain the half-maximal velocity. Although the concentration interval of ATP was not saturating at 0.5 and 1 mM Mn^{2+}, it appeared that the reaction velocities were approaching a similar maximum in all three curves. Therefore, within the concentration interval of Mn^{2+} that stimulated autophosphorylation (Fig. 9), the major effect of this cation was to decrease the apparent K_m for ATP.

The relation between the initial velocity of autophosphorylation and Mn^{2+} measured at various ATP concentrations is shown in Fig. 12, *center.* [Mn^{2+}] between 0.5 and 5.0 mM activated the receptor-kinase at all ATP levels tested; however, the concentration of Mn^{2+} required to activate the kinase decreased as the ATP concentration increased. Quantitative analysis of these hyperbolic velocity curves yielded the kinetic constants listed in Table II. The V_{max} increased sigmoidally with the ATP concentration to a limiting value of 160 ± 10 pmol/mg of protein/min which represents the maximum initial velocity of autophosphorylation at saturating concentrations of Mn^{2+}, ATP, and insulin. The corresponding K_m for ATP under these conditions was 19 ± 1 μM.

The K_m for Mn^{2+} decreased as the ATP concentration increased (Table II). Fig. 12, *right,* shows that the ratio, K_m (Mn^{2+})/V_{max}, which was calculated from the kinetic parameters in Table II and plotted against the reciprocal of the ATP concentration, was linear and extrapolated to the origin (slope ± S.E. = 782 ± 27 pmol/μM²/mg of protein/min). This result suggests that the K_m for Mn^{2+} approached zero as the ATP concentration increased to a saturating level. Therefore, in the intact cell where the ATP levels are relatively high and Mn^{2+} levels are relatively low (45), the receptor kinase should be active (1, 2).

DISCUSSION

Recent evidence suggests that the insulin receptor is a membrane-bound, tyrosine-specific protein kinase that is activated by insulin binding (1, 2, 4–16).[1] The purified receptor-kinase consists of two major subunits (30). The M_r = 135,000 (α) subunit is labeled covalently with insulin affinity reagents, a result which suggests that it contains the insulin binding domain (46, 47). The M_r = 95,000 (β) subunit of the receptor is the major site of autophosphorylation (1,2 4–8)[1] and is labeled specifically with ATP affinity reagents (14–16). These results suggest that it contains the catalytic domain of the kinase.

At least five sites of autophosphorylation can be identified by reverse-phase HPLC after trypsin digestion of the β-subunit. The phosphorylation of each site is stimulated by insulin. The autophosphorylation of two of these sites (pp4 and pp5) is complete after only 20 s of incubation with [γ-^{32}P]ATP and Mn^{2+}. At steady state, about 2 molecules of ^{32}P are incorporated per insulin binding site as estimated from a Scatchard plot. Assuming that the α- and β-subunit are associated in a stoichiometric ratio of 1:1 (46) and each α-subunit binds insulin (30), then about 2 molecules of ^{32}P are covalently bound to the β-subunit at steady state. However, these data do not imply phosphorylation of the β-subunit to an integral molar ratio because our results indicate that more than two phosphorylation sites exist on the molecule. This calculation of stoichiometry must be viewed cautiously for the following reasons: uncertainty remains about the subunit composition and stoichiometry of the intact insulin receptor (36); some denaturation of the α- or β-subunits may occur during receptor isolation (30); and the intact receptor may not bind more than 1 insulin molecule (48). Furthermore, the phosphorylation stoichiometry remains provisional because the amount of endogenous phosphorylation of the receptor isolated from the Fao cell is unknown. This variable may explain why all the sites of autophosphorylation do not reach the same level as well as why the amount of phosphorylation varies between preparations of insulin receptor.

Insulin stimulates autophosphorylation by increasing the V_{max} of ^{32}P incorporation 20-fold. All five major sites of phosphorylation in the β-subunit were stimulated by insulin. We have previously shown with the purified receptor kinase that insulin stimulates the V_{max} for substrate phosphorylation as measured with a synthetic tyrosine-containing peptide (8). These results suggest that insulin binding activates the recep-

tor kinase by causing a conformational change in the catalytic domain. However, it is possible that autophosphorylation is stimulated by an insulin-induced change which makes an important site of autophosphorylation more accessible to the catalytic domain. The resulting covalent modification may subsequently enhance the activity of the receptor-kinase toward other sites of autophosphorylation and exogenous substrates (26).

The kinetics of autophosphorylation for the various sites present in the β-subunit of the insulin receptor is not identical. Phosphorylation of pp4 and pp5 are very rapid, whereas pp1 and pp2 display a definite lag in the rate of phosphorylation. It is possible that the insulin-induced autophosphorylation of pp4 and pp5 stimulates the subsequent autophosphorylation of pp1 and pp2. Autophosphorylation of the β-subunit of the insulin receptor is slightly inhibited by concentrations of insulin greater than 100 nM (4, 7).[1] Our results suggest that this inhibition is due to a 50% decrease in the phosphorylation of pp2. It may be possible to establish a relation between the sites of autophosphorylation in the β-subunit and activation of the kinase with respect to substrate phosphorylation (26). To show a relation between the physiological insulin response and phosphorylation of the receptor at specific sites, it will be important to correlate the autophosphorylation sites observed *in vitro* with those observed *in vivo*.

In addition to insulin, regulation of the kinase may also occur by changing the concentration of divalent cations. Metal ions activate many enzymatic reactions by combining with both the enzyme and the substrate. Prototype examples of this reaction are the protein kinases which require ATP and Mg^{2+}, the active substrate being $MgATP^{2-}$ (49). Divalent metal ion activation of insulin receptor kinase autophosphorylation appears to be restricted *in vitro* to Mn^{2+} (6). This stimulation occurs predominantly by decreasing the K_m for ATP and is observed at concentrations of Mn^{2+} in excess of that necessary to form the presumed substrate, $MnATP^{2-}$. For example, at a Mn^{2+} concentration of 0.5 mM, assuming a dissociation constant for $MnATP^{2-}$ of 10 μM (50), the ATP calculated to be present as $MnATP^{2-}$ is between 97% and 98%. This relative distribution remains constant over the concentration interval of ATP used in these experiments. The increase in autophosphorylation observed at a constant concentration of ATP by increasing the concentration of Mn^{2+} from 0.5 to 5 mM, therefore, occurs without a major increase in the fraction of $MnATP^{2-}$. Since autophosphorylation of the receptor kinase is linear with respect to the concentration of protein used in the assay, it is unlikely that the solubilized receptor preparation nonspecifically complexes Mn^{2+}. Thus, activation of the insulin receptor kinase presumably requires binding of free Mn^{2+} to a specific site on the kinase, in addition to chelation of ATP^{4-} by Mn^{2+}. Since Mn^{2+} and Mg^{2+} form similar complexes with ATP (49, 50), the lack of any significant effect of Mg^{2+} in the presence or absence of Mn^{2+} also argues against the possibility that the stimulation of the kinase by Mn^{2+} occurs exclusively through chelation of ATP^{4-}, or by decreasing the concentration of uncomplexed inhibitory derivatives of ATP, such as $HATP^{3-}$ or ADP^{3-}. Our results are analogous to the selective stimulation by divalent cations on the hepatic adenylate cyclase system (51, 52). Since Mn^{2+} can play a dual role in activating the insulin receptor kinase, it is not surprising that a variety of complex kinetic curves are observed (42, 43). The sigmoidal relation between the velocity of autophosphorylation *versus* ATP concentration may reflect a complicated kinetic mechanism involving Mn^{2+}, allosteric effects, or activation by autophosphorylation.

The finding that the K_m for Mn^{2+} approached zero as the [ATP] increased suggests that Mn^{2+} binding precedes $Mn\text{-}ATP^{2-}$ binding by an equilibrium-ordered mechanism (42, 44). Another characteristic of this mechanism is that the V_{max} for the reaction is independent of the concentration of Mn^{2+} which seems to be the case for the receptor kinase. According to this hypothesis, the insulin receptor kinase will not bind ATP in the absence of a metal activator, presumably Mn^{2+}; however, the high level of ATP found in the intact cell (27) can drive the reaction to completion even in the presence of a very low level of the metal cation (42). Thus, the receptor kinase is active even when the activator concentration is low, provided that the substrate concentration is high.

Autophosphorylation of the partially purified insulin receptor is apparently independent of the protein concentration used in the assay. If a linear relation exists between the receptor kinase concentration and the initial rate of receptor phosphorylation, the 10-fold dilution of protein used in our experiments should be adequate to detect it. Insulin receptors could form aggregates in detergent solution which cause an apparent concentration independence of autophosphorylation; however, this possibility is unlikely because phosphorylation of the insulin receptor is independent of the Triton X-100 concentration. Owing to phosphatases which are present in the receptor preparation, dilution may cause fortuitously an equal decrease of autophosphorylation and dephosphorylation so that no net change is observed; however, this is unlikely because the *in vitro* dephosphorylation reaction is slow relative to the phosphorylation reaction.[1] The mechanism by which an intramolecular autophosphorylation reaction could occur at multiple sites is not clear.

Like the insulin receptor, other protein kinases undergo autophosphorylation at multiple sites by what appears to be an intramolecular reaction (27, 37, 38). The gene product of the Rous sarcoma virus, $pp60^{v\text{-}src}$, phosphorylates itself at Tyr in the COOH-terminal portion of the molecule *in vitro* (53). *In vivo*, $pp60^{v\text{-}src}$ is phosphorylated at serine and tyrosine residues (54). This finding is similar to the insulin receptor (1, 2). Recently, the major site of tyrosine autophosphorylation in $pp60^{v\text{-}src}$ was altered by constructing a mutant protein in which Tyr-416 was changed to a phenylalanine residue (55). This mutation had no effect on the transforming properties relative to wild type $pp60^{v\text{-}src}$ and no effect on the tyrosine kinase activity measured with exogenous substrates. However, another site of tyrosine autophosphorylation was detected in the COOH-terminal portion of the mutant molecule, so tyrosine autophosphorylation at this position may still be important for the biological activity of the kinase. Multiple sites of tyrosine phosphorylation in the epidermal growth factor receptor have been reported (56, 57), but their effect on the activity of the kinase is unknown. Autophosphorylation at serine residues of the regulatory subunit of the cAMP-dependent protein kinase from bovine cardiac muscle decreases the rate at which the active catalytic subunit reassociates with the regulatory subunit to form the less active holoenzyme (38, 58, 59). Therefore, this reaction appears to have a regulatory role. The catalytic activity of other serine kinases is also regulated by autophosphorylation (27).

The rapid autophosphorylation of the β-subunit suggests that the insulin receptor may translate the extracellular regulatory signal arising from insulin binding into an intracellular signal through the stimulation of tyrosine phosphorylation at the inner face of the plasma membrane. This regulatory signal, initiated by insulin binding, may be transmitted across the plasma membrane by stimulation of substrate phosphorylation of exogenous proteins at tyrosine residues. Alternatively, autophosphorylation itself may be a sufficient intracellular molecular signal to initiate the physiological

responses of insulin. In this model, signal transmission could occur without any additional phosphotransfer reactions if the phosphorylated receptor is modified in its ability to interact with relevant cytoplasmic or membrane-bound proteins.

In conclusion, we have shown that the insulin receptor has characteristic kinetic properties that may be important for insulin action. Both insulin and divalent cations affect the rate of autophosphorylation and may be important physiologic regulators of the membrane-bound kinase, but these act through different mechanisms. Autophosphorylation of the insulin receptor is a very rapid intramolecular reaction that may provide the link between extracellular insulin binding and a recognizable intracellular covalent modification.

REFERENCES

1. Kasuga, M., Karlsson, F. A., and Kahn, C. R. (1982) *Science* **215,** 185–187
2. Kasuga, M., Zick, Y., Blithe, D. L., Karlsson, F. A., Häring, H. U., and Kahn, C. R. (1982) *J. Biol. Chem.* **257,** 9891–9894
3. Deleted in proof
4. Häring, H.-U., Kasuga, M., and Kahn, C. R. (1982) *Biochem. Biophys. Res. Commun.* **108,** 1538–1545
5. Kasuga, M., Zick, Y., Blithe, D. L., Crettaz, M., and Kahn, C. R. (1982) *Nature (Lond.)* **298,** 667–669
6. Zick, Y., Kasuga, M., Kahn, C. R., and Roth, J. (1982) *J. Biol. Chem.* **258,** 75–80
7. Kasuga, M., Fujita-Yamaguchi, Y., Blithe, D. L., and Kahn, C. R. (1983) *Proc. Natl. Acad. Sci. U. S. A.* **80,** 2137–2441
8. Kasuga, M., Fujita-Yamaguchi, Y., Blithe, D. L., White, M. F., and Kahn, C. R. (1983) *J. Biol. Chem.* **258,** 10973–10980
9. Van Obberghen, E., and Kowalski, A. (1982) *FEBS Lett.* **143,** 179–182
10. Petruzzelli, L. M., Ganguly, S., Smith, C. R., Cobb, M. H., Rubin, C. S., and Rosen, O. (1982) *Proc. Natl. Acad. Sci. U. S. A.* **80,** 3237–3240
11. Machicao, F., Urumow, T., and Wieland, O. H. (1982) *FEBS Lett.* **149,** 96–100
12. Avruch, J., Nemenoff, R. A., Blackshear, P. J., Pierce, M. W., and Osathanondh, R. (1982) *J. Biol. Chem.* **257,** 15162–15166
13. Zick, Y., Whittaker, J., and Roth, J. (1983) *J. Biol. Chem.* **258,** 3431–3434
14. Roth, R. A., and Cassell, D. J. (1983) *Science* **219,** 299–301
15. Van Obberghen, E., Rossi, B., Kowalski, A., Gazzano, H., and Ponzio, G. (1983) *Proc. Natl. Acad. Sci. U. S. A.* **80,** 945–949
16. Shia, M. A., and Pilch, P. F. (1983) *Biochemistry* **22,** 717–721
17. Carpenter, G., King, L., Jr., and Cohen, S. (1979) *J. Biol. Chem.* **254,** 4884–4891
18. Cohen, S., Carpenter, G., and King, L., Jr. (1980) *J. Biol. Chem.* **255,** 4834–4842
19. Ushiro, H., and Cohen, S. (1980) *J. Biol. Chem.* **255,** 8363–8365
20. Pike, L. J., Gallis, B., Casnellie, J. E., Bornstein, P., and Krebs, E. G. (1982) *Proc. Natl. Acad. Sci. U. S. A.* **79,** 1443–1447
21. Erneux, C., Cohen, S., and Garbers, D. L. (1983) *J. Biol. Chem.* **258,** 4137–4142
22. Ek, B., Westermark, B., Wasteson, A., and Heldin, C.-H. (1982) *Nature (Lond.)* **295,** 419–420
23. Ek, B., and Heldin, C.-H. (1982) *J. Biol. Chem.* **257,** 10486–10492
24. Pike, L. J., Bowen-Pope, D. F., Ross, R., and Krebs, E. G. (1983) *J. Biol. Chem.* **258,** 9383–9390
25. Sefton, B. M., Hunter, T., Beemon, K., and Eckhart, W. (1980) *Cell* **20,** 807–816
26. Rosen, O. M., Herrera, R., Olowe, Y., Petruzelli, L. M., and Cobb, M. H. (1983) *Proc. Natl. Acad. Sci. U. S. A.* **80,** 3237–3240
27. Flockhart, D. A., and Corbin, J. D. (1982) *CRC Crit. Rev. Biochem.* **12,** 133–186
28. Deschatrette, J., Moore, E. E., Dubois, M., Cassio, D., and Weiss M. C. (1979) *Somat. Cell. Genet.* **5,** 697–718
29. Taylor, S., Hedo, J. H., Underhill, L. H., Kasuga, M., Eldus, M. J., and Roth, J. (1982) *J. Clin. Endocrinol. Metab.* **55,** 1108–1113
30. Fujita-Yamaguchi, Y., Choi, S., Sakamoto, Y., and Itakura, K. (1983) *J. Biol. Chem.* **258,** 5045–5049
31. Laemmli, U. K. (1970) *Nature (Lond.)* **227,** 680–685
32. Harrison, L. C., Flier, J. S., Roth, J., Karlsson, F. A., and Kahn, C. R. (1979) *J. Clin. Endocrinol. Metab.* **48,** 59–65
33. Van Obberghen, E., Kasuga, M., Le Cam, A., Hedo, J. A., Itin, A., and Harrision, L. C. (1981) *Proc. Natl. Acad. Sci. U. S. A.* **78,** 1052–1056
34. Hedo, J. A., Kasuga, M., Van Obberghen, E., Roth, J., and Kahn, C. R. (1981) *Proc. Natl. Acad. Sci. U. S. A.* **78,** 4791–4795
35. Kasuga, M., Kahn, C. R., Hedo, J. A., Van Obberghen, E., and Yamada, K. M. (1981) *Proc. Natl. Acad. Sci. U. S. A.* **78,** 6917–6921
36. Kasuga, M., Hedo, J. A., Yamada, K. M., and Kahn, C. R. (1982) *J. Biol. Chem.* **257,** 10392–10399
37. Rangel-Aldao, R., and Rosen, O. M. (1976) *J. Biol. Chem.* **251,** 7526–7529
38. Erlichman, J., Rangel-Aldao, R., and Rosen, O. M. (1983) *Methods Enzymol.* **99,** 176–186
39. Cleland, W. W. (1979) *Methods Enzymol.* **63,** 103–138
40. Allison, R. D., and Purich, D. L. (1979) *Methods Enzymol.* **63,** 3–22
41. Cleland, W. W. (1979) *Methods Enzymol.* **63,** 501–513
42. Segel, I. H. (1975) *Enzyme Kinetics,* pp. 227–272, John Wiley and Sons, New York
43. London, W. P., and Steck, T. L. (1969) *Biochemistry* **8,** 1767–1779
44. Morrison, J. F. (1979) *Methods Enzymol.* **63,** 257–294
45. Long, C. (1961) *Biochemist's Handbook,* D. Van Nostrand Co. Inc., Princeton, NJ
46. Yip, C. C., Yeung, C. W. T., and Moule, M. L. (1978) *J. Biol. Chem.* **253,** 1743–1745
47. Massagué, J., and Czech, M. P. (1982) *J. Biol. Chem.* **257,** 6729–6738
48. Pang, D. T., and Shafer, J. A. (1983) *J. Biol. Chem.* **258,** 2514–2518
49. Cleland, W. W. (1967) *Annu. Rev. Biochem.* **36,** 77–112
50. O'Sullivan, W. J., and Smithers, G. W. (1979) *Methods Enzymol.* **63,** 294–336
51. Londos, C., and Preston, M. S. (1977) *J. Biol. Chem.* **252,** 5951–5956
52. Londos, C., and Preston, M. S. (1977) *J. Biol. Chem.* **252,** 5957–5961
53. Smart, J. E., Oppermann, H., Czernilofsky, A. P., Purchio, A. F., Erikson, R. L., and Bishop, J. M. (1981) *Proc. Natl. Acad. Sci. U. S. A.* **78,** 6013–6017
54. Hunter, T., and Sefton, B. M. (1980) *Proc. Natl. Acad. Sci. U. S. A.* **77,** 1311–1315
55. Snyder, M. A., Bishop, J. M., Colby, W. W., and Levinson, A. D. (1983) *Cell* **32,** 891–901
56. Gates, R. E., and King, L. E. (1982) *Biochem. Biophys. Res. Commun.* **105,** 57–66
57. Cassel, D., Pike, L. J., Grant, G. A., Krebs, E. G., and Glaser, L. (1983) *J. Biol. Chem.* **258,** 2945–2950
58. Rangel-Aldao, R., and Rosen, O. M. (1976) *J. Biol. Chem.* **251,** 3375–3380
59. Rangel-Aldao, R., and Rosen, O. M. (1977) *J. Biol. Chem.* **252,** 7140–7145
60. Grigorescu, F., White, M. F., and Kahn, C. R. (1983) *J. Biol. Chem.* **258,** 13708–13716

Supplemental Material to

KINETIC PROPERTIES AND SITES OF AUTOPHOSPHORYLATION OF THE PARTIALLY PURIFIED INSULIN RECEPTOR FROM HEPATOMA CELLS

Morris F. White, Hans-Ulrich Häring, Masato Kasuga, and C. Ronald Kahn

EXPERIMENTAL PROCEDURES

Materials - The following materials were obtained from the sources indicated: [γ-^{32}P]ATP and Triton X-100 were from New England Nuclear; HEPES, aprotinin, phenylmethylsulfonyl fluoride, N-acetylglucosamine, bovine serum albumin and bovine gamma globulin were from Sigma; trifluoroacetic acid, trichloroacetic acid, polyethylene glycol (PEG 6000), and HPLC grade acetonitrile, were from Fisher Scientific; L-1-tosylamido-2-phenylethyl-chloromethyl ketone (TPCK) treated trypsin was from Worthington; porcine insulin was from Elanco; reagents for SDS-PAGE and the Bradford protein assay were purchased from Bio-Rad; Pansorbin and Bacitracin were from Calbiochem; wheat germ agglutinin-agarose was from Vector. [^{125}I-Tyr^{A14}]monoiodoinsulin was prepared in our laboratory (60).

Cell Culture - The hepatoma cell (Fao) line was obtained from Dr. M.C. Weiss (Guf-sur-Yvette, France). The Fao cell line is a fourth generation clonal line of well differentiated rat hepatoma cells derived from the Reuber H-35 hepatoma (28). It has many insulin receptors and is very sensitive to insulin as measured by stimulation of glycogen synthase and tyrosine aminotransferase activities [Crettaz, M., and Kahn, C.R, unpublished results]. Monolayer cultures of Fao cells were grown to confluence in 150 cm^2 plastic dishes (Nunc) or plastic bottles (Corning) containing 50 ml of Coon's modified F12 medium (GIBCO) supplemented with 5% fetal bovine serum (Hyclone), 100 units/ml penicillin (GIBCO), and 100 µg/ml streptomycin (GIBCO).

Solubilization and Purification of the Insulin Receptor - Sixty confluent dishes of hepatoma cells were washed at 22°C with 20 ml of normal saline buffered with 25 mM phosphate at pH 7.4. Two ml of solubilization buffer composed of 1% Triton X-100, 25 mM HEPES at pH 7.4, aprotinin (1000 trypsin inhibitor units/ml) and 2 mM PMSF were added to each dish. The cells were scraped from the dishes into conical test tubes and mixed by vortexing. Aliquots (10 ml) of this mixture were transfered to ultracentrifugation tubes (Beckman) and the detergent insoluble material was sedimented by centrifugation at 50,000 rpm in a Beckman 70 Ti rotor for 40 min. The supernatant from each tube was combined and diluted 1:1 with a solution of 25 mM HEPES (pH 7.4) to give a final volume of about 200 ml. This solution was passed over a 2 ml wheat germ agglutinin-agarose column and the effluent flowed directly onto a second identical column. After sample application, each column was washed separately with 200 ml of a solution containing 0.1% Triton X-100 and 25 mM HEPES (pH 7.4). Finally each column was eluted separately with 5 ml of this solution supplemented with 300 mM N-acetyl-glucosamine. The protein-containing fractions determined with the Bradford assay standardized with bovine serum albumin (Bio-Rad) were pooled (3 ml from each column), separated into 250 µl aliquotes containing 100 µg of protein per ml, and stored at -70°C for 3 months without apparent loss of autophosphorylation activity.

Insulin binding to the Solubilized Insulin Receptor - Insulin binding was carried out as described previously (29). Solubilized insulin receptor (5 µg) was incubated with [^{125}I]monoiodo-insulin (10,000 cpm) in a buffer containing 0.05 mM HEPES, pH 7.8, 0.15 mM NaCl, 0.1% bovine serum albumin, 0.1% Triton X-100, and bacitracin (100 units/ml) in the presence of varying concentrations of unlabeled porcine insulin. The final assay volume was 0.2 ml. Incubations were carried out at 4°C for 16 h, then the receptor was precipitated by addition of 0.3 ml of polyethylene glycol (25% wt/vol) and 0.1% bovine gamma globulin (3 mg/ml). The amount of insulin bound to the precipitated receptor at each insulin concentration was determined in triplicate.

The total insulin binding capacity of our preparation of insulin receptor, estimated from the abscissa intercept of a curvilinear Scatchard plot, was about 100 pmol of insulin per mg of protein (Fig. 1). Assuming a M_r = 350,000 for the native insulin receptor which contains two insulin binding sites (30), this value corresponds to about 2% of the theoretical specific insulin binding activity of the pure insulin receptor.

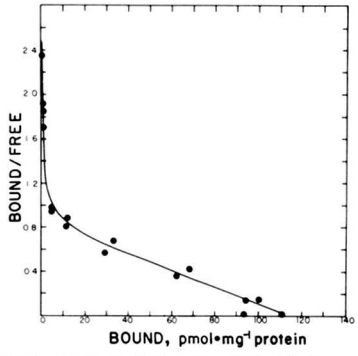

FIGURE 1. A Scatchard plot of insulin binding to the solubilized insulin receptor.

Phosphorylation Assay - Solubilized insulin receptor (3 to 4 µg) was diluted to 50 µl (60 to 80 µg of protein per ml) and adjusted to contain a final concentration of 100 mM HEPES, pH 7.4, and 0.1% Triton X-100. Insulin and Mn^{2+} were added at concentrations indicated in the figure and table legends and this solution was incubated at 22°C for 1 h. Then 5 µl of 10-fold concentrated [γ-^{32}P]ATP (24,000 - 54,000 counts per min per pmol) were added, the mixture was vortexed, and the incubation was continued for variable time intervals at 22°C. The reaction was terminated by adding 10 µl of 5-fold concentrated Laemmli sample buffer to obtain final concentrations of the following components: 2% SDS, 0.1 M dithiothreitol, 0.01% bromphenol blue, 10% glycerol, and 10 mM sodium phosphate at pH 7.0 (31). This mixture was heated immediately in a boiling water bath for 3 min. The proteins were separated by sodium dodecylsulfate polyacrylamide gel electrophoresis (SDS-PAGE) using 4.0% stacking and 7.5% resolving polyacrylamide gels according to the method of Laemmli (31). Proteins were fixed and stained in the polyacrylamide gels during a 5 min incubation at room temperature with 50% trichloroacetic acid containing 0.2% Coomassie Blue. The gels were destained at 37°C for 12 h in 7% acetic acid and dried in vacuo for 1 h at 80°C.

In the case where the insulin receptor was immunoprecipitated, the phosphorylation reaction was stopped by cooling the mixture to 4°C and adding 20 µl of a "stopping" solution to obtain a final concentration of 5 mM ATP, 5 mM EDTA, 100 mM sodium fluoride, and 10 mM sodium pyrophosphate (2). Anti-insulin receptor antibody (B-8) was added to this mixture at a dilution of 1:300 and incubated at 4°C for 2 h as previously described (32-35). The immune complex was precipitated from the solution on Pansorbin (36). The protein in the supernatant and the immunoadsorbed protein was solubilized in Laemmli sample buffer containing DTT and applied on the gel.

The radioactivity located in gel fragments by autoradiography was quantified by scintillation counting in 5 ml of 3a70b scintillation mixture (Research Products International Corp.). The background radiation was estimated by measuring the radioactivity in a gel fragment of the same size shown by autoradiography to be free of discrete bands of phosphoprotein.

Identification of the Phosphorylated Insulin Receptor - Insulin receptors solubilized with Triton X-100 from Fao hepatoma cells and purified on wheat germ agglutinin agarose exhibit insulin-stimulated autophosphorylation which occurs exclusively on tyrosine residues of the β-subunit (2). During previous studies, we have relied on specific immunoprecipitation by anti-insulin receptor antibodies to identify the phosphorylated receptor (2). However, rapid quenching of the reaction mixture with Laemmli sample buffer (31) at 100°C was necessary for an accurate analysis of the initial velocity of the autophosphorylation reaction. Unfortunately, the denaturation of proteins caused by this procedure precludes the use of immunoprecipitation. Therefore, it was important to demonstrate that autophosphorylation of the partially purified insulin receptor could be studied without immunoprecipitation. Separation of the proteins from a portion of the standard reaction mixture by SDS-PAGE under reducing conditions before immunoprecipitation (Fig. 2, lanes a and d) revealed that insulin (100 nM) stimulated the incorporation of ^{32}P into a single protein that migrated with M_r = 95,000. This phosphoprotein was almost completely precipitated by an antibody to the insulin receptor (Fig. 2, compare lanes c and f to lanes b and e) suggesting that the M_r = 95,000 band was the β-subunit of the insulin receptor. In some experiments, a second insulin-stimulated phosphoprotein of M_r = 135,000 was also present in the immunoprecipitated receptor (Fig. 2, lanes c, f). This protein may be the α-subunit of the insulin receptor (6), but was not detected reproducibly in our experiments with the Fao cells.

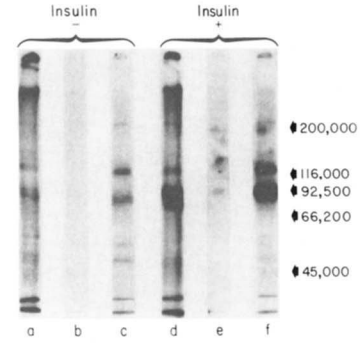

FIGURE 2. An autoradiogram showing the identification of the solubilized, phosphorylated insulin receptor by immunoprecipitation. Insulin receptor (4 µg) was incubated for 10 min at 20°C without insulin (lanes a-c) or with 100 nM insulin (lanes d-f). Half (25µl) of each reaction mixture (lanes a and d) was stopped by heating it in the presence of Laemmli sample buffer. The proteins were separated by SDS-PAGE under reducing conditions without immunoprecipitation. The remainder of the reaction (25 µl) was cooled to 4°C and mixed simultaneously with 25 µl of stopping solution containing 200 mM NaF, 10 mM ATP, 10 mM EDTA and 20 mM sodium pyrophosphate. This mixture was immunoprecipitated with anti-insulin receptor antibodies and the supernatant (lanes b and e) and the precipitate (lanes c and f) were separated by SDS-PAGE.

Tryptic Peptide Mapping by High Performance Liquid Chromatography - Fixed, stained, destained, and dried polyacrylamide gel fagments containing phosphoprotein located by autoradiography were washed for 12 h at 37°C with 20 ml of 10% methanol. The adsorbent paper was removed from the gel fragment. The gel was dried at 70°C for 60 min and rehydrated in 2 ml of 50 mM NH_4HCO_3 containing 100 µg of TPCK treated trypsin. This mixture was incubated for 24 or 48 h at 37°C, the gel fragment was removed and the supernatant was clarified by centrifugation. If a 48 h digestion was used, 100 µg of fresh trypsin was added to the reaction solution after the first 24 h of incubation. The supernatant was lyophilized and the residue was dissolved in 25 - 50 µl of 0.1% trifluoroacetic acid. The phosphopeptides were separated using a Waters high performance liquid chromatography system equipped with a µBondapak C_{18} reversed-phase column. Phosphopeptides applied to the column were eluted at a flow rate of 1 ml/min with water containing 0.05% trifluoroactic acid and modified with acetonitrile also containing 0.05% trifluoroacetic acid. Radioactivity in 0.4 ml to 1.0 ml fractions eluted from the reversed-phase column was measured in 5 ml of scintillation mixture.

Trypsin digestion of the phosphorylated β-subunit suggested that at least 5 peptides containing sites of ^{32}P incorporation exist in this molecule which eluted with retention times between 20 to 35 min (Fig. 2). The pattern of phosphopeptide elution was similar after 24 and 48 h of incubation with trypsin suggesting that maximum digestion was attained after 24 h. These phosphopeptides were reproducibly identified during the course of this study, whereas the fragments having longer retention times were not reproducibly detected, and were usually minor. We have focused our attention on the 5 major phosphopeptides released after 24 h of trypsin digestion and have arbitrarily numbered them pp1 - pp5 for purposes of identification.

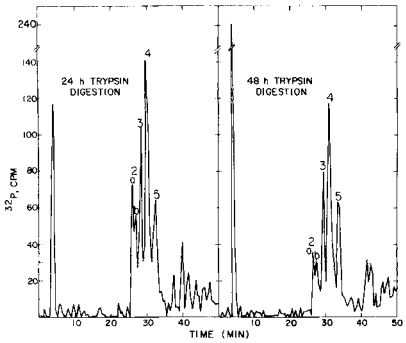

FIGURE 3. Trypsin digestion of the β-subunit of the insulin receptor. Insulin receptor (4 μg) was phosphorylated during 1 min in a mixture containing 100 nM insulin, 50 μM [γ-^{32}P]ATP, and 5 mM Mn^{2+}. The polyacrylamide gel fragment identified by autoradiography to contain the phosphorylated β-subunit was excised and incubated with trypsin for 24 h. (Left) The phosphopeptides contained in half of this supernatant were separated by HPLC. (Right) Fresh trypsin was added to the remainder of the sample and this mixture was incubated at 37°C for an additional 24 h then the phosphopeptides were separated by HPLC. The acetonitrile gradient used was 0% (5 min) and 0%-70% (75 min).

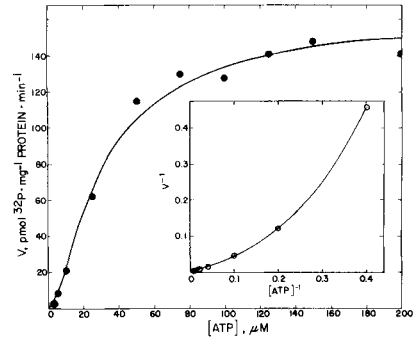

FIGURE 8. A kinetic curve of insulin receptor autophosphorylation. Solubilized insulin receptor (3.4 μg) was incubated with 100 nM insulin and 5 mM Mn^{2+} for 1 h followed by the addition of the indicated concentrations of [γ-^{32}P]ATP for 30 s. The reaction was terminated by heating to 100°C for 2 min and the proteins were separated by SDS-PAGE. The phosphorylated β-subunit of the insulin receptor was identified by autoradiography and the radioactivity in the corresponding gel fragment was quantitated by scintillation counting. The inset shows the corresponding Lineweaver-Burk plot. The kinetic parameters, K_m = 36 ± 2 μM and V_{max} = 171 ± 10 nmol/mg protein·min were determined by fitting these data to Eq. 2.

RESULTS

Measurement of the Kinetic Parameters for ATP and Mn^{2+} - Initial velocity kinetic data obtained for the phosphorylation of the β-subunit was analyzed statistically using a nonlinear least-squares analysis. Where appropriate, attempts were made to fit the data using one of the following equations described by Cleland (39):

1. Hyperbolic Velocity Curve

$$\log v = \log \left[\frac{V_{max} \cdot [S]}{K_m + [S]} \right]$$

2. Sigmoidal Velocity Curve

$$\log v = \log \left[\frac{V_{max} \cdot [S]^2}{a + 2b[S] + [S]^2} \right]$$

3. Substrate inhibition

$$v = \frac{V_{max} \cdot [S]}{K_m + [S] + [S]^2/K_i}$$

The initial velocity of insulin receptor autophosphorylation was estimated during a 30 sec time interval at 22°C in the presence of 100 nM insulin, 5mM Mn^{2+}, and a range of [γ-^{32}P]ATP concentrations between 2.5 and 200 μM. The sigmoidal relation between the reaction velocity and the ATP concentration, and the corresponding parabolic Lineweaver-Burk plot are shown in Fig. 8. The sigmoidal shape of the velocity curve was confirmed by statistical analysis using Eq. 1 and Eq. 2. The values of K_m ± S.E. for ATP and V_{max} ± S.E. for autophosphorylation using the equation for a sigmoidal curve (Eq. 2) were 36 ± 2 μM and 171 ± 10 pmol/mg protein·min, respectively; the square root of the residual least square was 0.068. By comparison, the corresponding values obtained by fitting these data to the hyperbolic velocity equation (Eq. 1) were 209 ± 150 μM, 380 ± 219 pmol/mg protein·min, and 0.37, respectively. The latter set of values indicate an inferior fit owing to the larger relative standard errors and larger value of the square root of the sum of residual least squares (39). Apparent sigmoidal kinetic curves can arise if the time intervals used are not good estimates of the initial rate of phosphorylation (40); however, the 30 sec time interval used for the experiment shown in Fig. 8 appears to be in the linear phase (Fig. 5A).

Under the conditions of our autophosphorylation assay, Mn^{2+} is an essential activator of the insulin receptor-kinase. When the partially purified receptor stimulated with insulin was incubated for 1 min with 50 μM ATP at room temperature, 5 mM Mn^{2+} maximally stimulated autophosphorylation, whereas higher concentrations of this divalent cation inhibited the reaction (Fig. 9). No phosphorylation was detected in the absence of Mn^{2+} or when Mg^{2+} at concentrations between 0.2 to 40 mM was substituted for Mn^{2+} (data not shown). The inhibition of autophosphorylation by high concentrations of Mn^{2+} was emphasized by the nonlinear double reciprocal plot shown in the inset to Fig. 9. This type of curve indicates the occurence of substrate inhibition (41). Therefore, analysis of these data was carried out using Eq. 3 which yielded values for K_m (Mn^{2+}) and V_{max} for autophosphorylation of 3.6 ± 1 mM and 178 ± 44 pmol/mg protein·min, respectively. The corresponding inhibition constant, K_i, for Mn^{2+} was 16 ± 8 mM. Therefore at [Mn^{2+}] below 5 mM the autophosphorylation reaction is approximately hyperbolic.

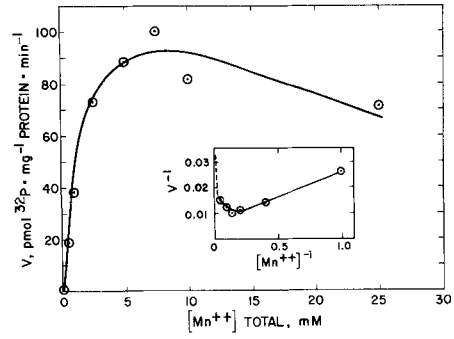

FIGURE 9. Mn^{2+} Stimulates and Inhibits Autophosphorylation of the Insulin Receptor. Solubilized insulin receptor (3.4 μg) was incubated with 100 nM insulin and the concentrations of Mn^{2+} indicated on the abscissa for 1 h followed by the addition of 50 μM [γ-^{32}P]ATP for 1 min. The reaction was terminated and the proteins were separated by SDS-PAGE. The phosphorylated β-subunit of the insulin receptor was identified by autoradiography and the radioactivity in the corresponding gel fragment was quantitated by scintillation counting. The inset shows the corresponding Lineweaver-Burk plot. Statistical analysis of these data by using Eq. 3 yields the following values for the kinetic parameters ± S.E.: K_m (Mn^{2+}) = 3.6 ± 1 mM, V_{max} = 178 ± 44 pmol ^{32}P per mg of protein per min, and K_i (Mn^{2+}) = 16 ± 8 mM.